

## Impact of fouling, cleaning and faecal contamination on the separation of water from urine using thermally driven membrane separation

F. Kamranvand<sup>a</sup>, C.J. Davey<sup>a</sup>, H. Sakar<sup>a,b</sup>, O. Autin<sup>a</sup>, E. Mercer<sup>a</sup>, M. Collins<sup>a</sup>, L. Williams<sup>a</sup>, A. Kolios<sup>a</sup>, A. Parker<sup>a</sup>, S. Tyrrel<sup>a</sup>, E. Cartmell<sup>a</sup>, E.J. McAdam<sup>a,\*</sup>

<sup>a</sup>Cranfield Water Science Institute, Vincent Building, Cranfield University, Bedfordshire, MK43 0AL, UK

<sup>b</sup>Environmental Engineering Department, Gebze Technical University, Gebze, 41400, Turkey

\*Corresponding author e-mail: e.mcadam@cranfield.ac.uk

### Abstract

In this study, membrane distillation is evaluated as a technology for non-sewered sanitation, using waste heat to enable separation of clean water from urine. Whilst membrane fouling was observed for urine, wetting was not evident and product water quality met the proposed discharge standard, despite concentration of the feed. Fouling was reversible using physical cleaning, which is similar to previous membrane studies operating without pressure as the driving force. High COD reduction was achieved following faecal contamination, but mass transfer was impeded and wetting occurred which compromised permeate quality, suggesting upstream intervention is demanded to limit the extent of faecal contamination. (100 words)

**Running head:** Membrane distillation for urine treatment (41 characters with spaces)

**Keywords:** Faecal, source separation, membrane distillation, vacuum, water quality

## 1. Introduction

Economic losses of US\$260 billion have been attributed to the impact of poor sanitation and water in developing countries which underpins the need for considerable investment in infrastructure (1). However, to achieve in-house piped water supply and sewerage connection with partial treatment of sewage would require investment of US\$136.5 billion per year (2), which suggests that intervention through conventional, capital intensive, large-scale networked water and wastewater treatment assets, may not be economically feasible. It is also important to note that partial treatment of sewage does not necessarily mean safe sanitation, the impacts of which include an estimated one million preventable deaths per year, primarily from dysentery-like diarrheal diseases (3).

In response to this significant challenge, the Water, Sanitation & Hygiene program of the Bill & Melinda Gates Foundation initiated the Reinvent the Toilet Challenge in 2011 to promote the development of sustainable sanitation systems which provide safe, affordable sanitation that can operate independent of networked utilities. The Nano-Membrane Toilet (NMT) is one such solution under development which seeks to provide safe sanitation at a single household scale (around ten residents), without dependency on grid produced electricity, in order to increase operational resilience in areas with intermittent supply (4). Briefly, the NMT facilitates post-flush source-separation through a combination of gravity separation and screw extrusion to yield two phases, a faecal solids fraction (around 0.25 L per person per day) and a faecally contaminated liquid fraction (around 1.5 L per person per day) (5). Small-scale combustion of the faecal solids fraction at temperatures up to 600°C has been successfully demonstrated which ensures pathogen destruction, but also enables recovery of high grade heat which can be deployed to power the overall system (4)(6).

The liquid fraction is considerably more concentrated than blackwater due to the absence of flush-water (7), and so comprises mostly of urine, which is faecally contaminated. The extent of this contamination is dependent upon the residence time and mixing profile introduced before phase

separation (8), but will inevitably increase the organic (particulate, colloidal and soluble), inorganic and pathogenic composition. Regardless of the load applied to the downstream separation technology, the final liquid product should satisfy the criteria in the proposed ISO standard on 'Non-Sewered Sanitation Systems', to ensure safe discharge into the environment (3).

Membrane technology has been demonstrated as an effective barrier technology for off-grid application, which can be configured to require minimal energy demand. For example, gravity driven dead-end ultrafiltration (100 nm pore size) has been demonstrated to provide good pathogen retention during the treatment of stored urine and for the treatment of raw water contaminated by combined sewer overflow, but delivers only poor chemical oxygen demand (COD) and nutrient separation which is required to meet the proposed discharge standards (9)(10). Due to the availability of high grade heat, a vapour pressure gradient can instead be introduced to provide an energy efficient driving force for separation. In membrane distillation (MD), a hydrophobic membrane facilitates the diffusion of water vapour through the porous structure from the heated feed to the condensate side (11). Consequently, the membrane can provide analogous physical size exclusion properties to conventional membranes, including viable but non-culturable bacteria (12), but provide additional selectivity through vapour transport. Zhao et al. (13) demonstrated such selectivity, reporting >99% COD separation from urine using vacuum driven MD. Tun et al. (14) instead concentrated ammonia nitrogen within source separated urine by favouring water transport through direct contact MD. Whilst these few studies, together with the successful use of MD for water reclamation from urine in European Space Stations (15), demonstrates conceptual viability, there remains limited evidence in the literature regarding the impact of fouling or faecal contamination which will inevitably present operational challenges at the decentralised scale. The aim of this study is therefore to study membrane distillation as an enabling technology for non-sewered sanitation, to provide high quality water separation from faecally contaminated urine using waste heat. Specific objectives are to: (i) evaluate fouling phenomena promoted during urine separation; (ii) profile separation efficiency during treatment of real fluids; (iii) establish productivity

recoverability following fouling; and (iv) determine the impact of faecal contamination on separation efficiency and water productivity.

## 2. Material and methods

### 2.1 Experimental set-up

Feedwater temperature was sustained at 60 °C by placing within a heated water bath, and was enclosed to limit sample evaporation. Feedwater was recirculated from the heated bath to the membrane cell using a peristaltic pump (520U, Watson Marlow, Falmouth, UK) at a fixed flow rate (400 mL min<sup>-1</sup>) to sustain a crossflow velocity of 0.1 m s<sup>-1</sup> over the membrane surface (Figure 1). The Perspex membrane cell comprised of a single hollow fibre membrane sited within a channel (*w*, 0.012 m; *h*, 0.006m). The hollow-fibre membrane was constructed of microporous polytetrafluoroethylene (PTFE) with an inner and outer diameter of around 1.5 and 1.9 mm, and a wall thickness of around 190 µm (Figure 2) (Markel, USA). Average pore size characteristics were estimated through microscopic investigation, which suggested typical pore length and pore width of 3µm and 0.18µm respectively, using the mode. The probability for membrane wetting can be estimated using (16):

$$\Delta P_{B.P.} = \frac{-4B\gamma\cos\theta}{d_{max}} \quad (1)$$

where *B* is pore geometry coefficient, *d*<sub>max</sub> is pore size (m) and *γ* is surface tension (mN m<sup>-1</sup>). The active membrane length was 0.21m (effective surface area, 10 cm<sup>2</sup>). Based on the pore size measurements undertaken, the *B* co-efficient for this membrane was 16.7.

A glass viewing window was inserted into the top of the cell, to allow for real-time imaging with a microscope (Leica DM5500B Microsystems, Milton Keynes, UK) (17). Vacuum was introduced on the lumen-side by vacuum pump (N920 Series, KNF Neuberger Inc., NJ, US), and pressures monitored on both feed and permeate side (PXM319-001AI and PXM319-001GI, Omega Ltd., Manchester, UK). Permeate was collected using a cold temperature condenser (2 °C) and the mass of permeate measured over time using a balance (PR410 Symmetry, Cole-Parmer Ltd., London, UK).

## 2.2 Feed-water preparation, pre-treatment and membrane cleaning

Synthetic urine was prepared with reference to the characterisation of human urine presented by Putnam (20), to include: *inorganic salts* (Sodium Chloride, Potassium Chloride, Potassium Phosphate, Potassium Sulphate, Magnesium Sulphate, Magnesium Carbonate, Calcium Phosphate), *organics salts* (Creatinine, Creatine, Glycine, Glucose, Tyrosine), *ammonium salts* (Ammonium Hippurate, Ammonium Citrate, Ammonium Lactate, Ammonium Formate, Ammonium Oxalate) and *Urea*. Real human urine was collected daily, and used directly without dilution or pre-treatment. Faecally contaminated urine was prepared by mixing real urine with human faeces at a volumetric ratio of 7:1, which is representative of daily volumetric human production. The faecally contaminated urine was subject to vortex mixing for 30 seconds to provide a solution representative of the highest achievable faecal contamination. Prior to use, large particles were removed through coarse filtration with cotton wool and sand, to limit pipe clogging. The reversibility of membrane fouling was first studied with physical cleaning (deionised water rinse) followed by chemical cleaning comprising an acid wash (Citric acid at pH 3), alkaline wash (NaOH at pH 10) and finally deionised water wash. Ethics approval for the anonymous collection of faeces and urine was obtained through the Cranfield University Research Ethics System (CURES: 2310/2017; 2407/2017).

## 2.3 Analytical methods

Ammonium ( $\text{NH}_4^+\text{-N}$ ) and COD were measured using spectrophotometry (Spectroquant® cell tests, Merck). Solution pH and conductivity were determined with pH probe (4330, Jenway, Stone, UK) and conductivity meter (Mettler Toledo, Leicester, UK) respectively. The concentration of creatine, creatinine and urea were quantified using colorimetric assays (Sigma Aldrich, Poole, UK) and the light absorbance determined with a microplate reader (Tecan Infinite 200 PRO, Männedorf, Switzerland). Fouled membrane fibres were imaged using a scanning electron microscope (SEM) (XL30, FEI, Hillsboro, Oregon, USA) equipped with a field emission gun (sFEG) (XL30, FEI, Hillsboro,

Oregon, USA). Membrane samples were coated with gold–palladium (Au–Pd) using a cool sputtering SEM coating unit (E5100, Polaron Equipment/Quorum Technologies Ltd., Lewes, UK). Liquid surface tension was determined with a DuNoüy ring tensiometer (K6, Kruss, Bristol, UK), which was calibrated using deionised water ( $72.8 \text{ mN m}^{-1}$ ).

### **3. Results**

#### *3.1 Comparison of water productivity and rejection properties using synthetic and real urine*

Water productivity was initially evaluated using synthetic urine comprised of the critical inorganic and organic constituents (20). A slow decline in flux was observed at the outset of the experiment (0 to 25 h), followed by the onset of a ‘steady-state’ flux; the intermediate rise in flux was due to slow drainage at the condenser (Figure 3). Membrane rejection analysis was undertaken to discretise the influence of urine constituents (Table 1). Whilst the additive effect of the constituents increased initial feed concentration, the membrane achieved consistently high rejection of salts, COD and ammonium. An analogous trend in water productivity was demonstrated with real urine, where an initial gradual decline in productivity was followed by a period of relative ‘steady-state’. Real urine composition was similar to the synthetic and separation of salts, COD and ammonium were >98%, >98% and >92% respectively (Table 1). For real urine, urea, creatine and creatinine were also quantified and a rejection >98% recorded. Whilst ostensibly similar rejection profiles and water productivities were achieved for the synthetic and real urine, real-time images of the polarised layer developing adjacent to the membrane surface, indicate quite different fouling behaviour (Figure 4). Analysis of the deposit formed with real urine using SEM (Figure 5) coupled with energy dispersive x-ray diffraction, evidenced a deposit rich in carbon, phosphorous, and calcium (C, 21.3; ; P, 9.5; ; Ca, 11.3 %).

#### *3.2 Membrane cleaning strategies following the treatment of real urine*

Following the diminution in water productivity, cleaning protocols were trialled to ascertain the efficacy of flux restoration (Figure 6). An initial physical clean was initiated after 43 h operation, comprising physical rinsing with deionised water. The used cleaning solution was characterised by conductivity and COD of  $2190 \mu\text{S cm}^{-1}$  and  $772 \text{ mg l}^{-1}$  respectively; this indicates reversible organic deposition of  $6.8 \text{ gCOD m}^{-2}$  (Table 2). Once re-started, initial water flux was fully restored and similar to the virgin fibre, the temporal water productivity profile was characterised by a slow decrease in flux, followed by a rapid decrease in flux commencing around 40h after filtration. Both physical and acid/base chemical cleaning was initiated. The initial DI rinse characteristics were similar to the initial physical clean; the concentration of the chemical rinse fractions being lower in concentration (Table 2). Once again initial flux was restored and an analogous water productivity profile presented. Comparison of membrane rejection characteristics throughout each operational cycle were similar (Table 3).

### 3.3 *Establishing the impact of faecally contaminated urine on water productivity and selectivity*

A marked reduction in water productivity was noted in the early stages of permeation (0 to 5 h) when faecally contaminated urine was introduced as the feedwater (Figure 7). As with real urine, a steady-state flux was achieved, but this was markedly below the productivities of either clean water or real urine. As with the literature (21), surface tension of the urine and faecally contaminated urine were markedly below clean water ( $72.8 \text{ mN m}^{-1}$ ) at around 56 and  $52 \text{ mN m}^{-1}$  respectively (Figure 8). This is equivalent to an estimated reduction in membrane breakthrough pressure of between 23 and 28% versus the synthetic urine (Eq. 1).

During longer term operation with real urine, the temporal profile for permeate conductivity, COD and ammonia concentration were consistent, with COD and ammonia recorded below the proposed ISO discharge consent (Figure 9). In comparison, whilst an initial steady-state permeate concentration was also observed for faecally contaminated urine, the quality was considerably lower than for urine. A further reduction in permeate quality was evidenced for conductivity, COD and

ammonia after around 80h of permeation. This rapid decline in permeate quality corresponded to a concentration factor ( $C_f = c_f/c_i$ ) of around 1.32, whereas a  $C_f$  exceeding 1.5 was achieved with urine before permeation was arbitrarily stopped and did not evidently influence permeate quality.

#### 4. Discussion

In this study, a thermally driven membrane process has been demonstrated for the separation of high quality product water from urine and the resilience to faecal contamination and membrane surface fouling further evaluated. High rejection of inorganic and organic compounds was evidenced when separating water from synthetic urine (Table 1) which has been previously demonstrated with hydrophobic microporous membranes when applied to synthetic brine concentrate with initial conductivity ranging 22.9 to 44.9 mS cm<sup>-1</sup> (22). For real urine, surface tension was reduced by around  $\Delta\gamma$  20 mN m<sup>-1</sup> compared to synthetic urine (around 25%, Figure 8). Mills et al. (21) attributed the low surface tension to surface active bile acids which were absent in the synthetic urine composition (20). The reduction in surface tension is proportional to a reduction in breakthrough pressure, indicating an increased probability for membrane wetting (Figure 8, (16)). The hydrophobicity of the membrane implies that prior to wetting only volatiles can pass through (12). The rejection profile during real urine treatment was ostensibly similar to synthetic urine suggesting limited membrane wetting occurred. This was confirmed by the poor transmission of urea (<0.01%), a non-volatile solute, through the microporous membrane used. For comparison, Cath et al. (23) demonstrated urea (MW, 60.06 g mol<sup>-1</sup>) to be poorly rejected by reverse osmosis membranes, which provides further demonstration of the effective separation provided by thermally driven membrane technology.

For both synthetic and real urine, an initial flux decay was observed at the outset of permeation, followed by the onset of a period of steady-state, despite the deposition noted on the membrane surface through direct observation (Figure 4). The attainment of steady-state flux is similar to earlier studies that have applied MD to complex wastewaters (12)(14). Following a period



of steady-state, a considerable flux decline was noted, which did not influence permeate product quality (Figure 6, Table 1). Gryta et al. (24) noted complete membrane coverage through organic deposition following treatment of saline meat processing wastewater, and similarly noted no impact on product water quality. Whilst the fouling layer is likely to confer both mass and heat transfer hindrance, it has been proposed that the vapour pressure resistance of the fouling layer is negligible, and it is mass transfer resistance which is responsible for the lower flux observed (25). In this study, a predominantly crystalline deposit was ostensibly formed with synthetic urine (Figure 4). Whilst dendritic crystals were observed within the fouling layer formed with real urine (Figure 5) which can be ascribed to the precipitation of inorganic calcium phosphate ( $S_{Ca_3PO_4} 20 \text{ mg l}^{-1}$ ; (26)), a more complex deposit was formed, comprising a rich organic fraction exceeding  $4600 \text{ mgCOD m}^{-2}$  (Figure 4, Table 2). For illustration, Metzger et al. (27) observed deposition of around  $350 \text{ mg m}^{-2}$  protein and carbohydrate on an ultrafiltration membrane within a membrane bioreactor (MBR) that was sufficient to impede permeability. Whilst DI water seemingly recovered flux within the first cleaning cycle, visual discolouration of the membrane following the first physical clean indicated that some irrecoverable fouling will develop. Consequently, in the second cleaning cycle, a chemical clean was combined with the physical clean to quantify the recovered material in the washing fractions. Inclusion of physical/chemical intervention restored operational flux almost completely (Figure 6), which is indicative of non-specific reversible membrane fouling, and also provides demonstration PTFE membrane compatibility with such protocols. The reversibility may in part be accounted for by the lack of hydraulic pressure across the membrane which minimises the associative convective force in comparison to conventional ultrafiltration application, a concept which has been similarly observed in osmotic MBR (28) (29).

A marked decline in initial flux was observed following introduction of faecally contaminated urine (Figure 7). Tun et al. (14) also observed lower flux and faster flux decay with source separated urine in comparison to urine, attributing the flux decline to the presence of suspended solids (presumably of faecal origin). In this study, the extent of faecal contamination was comparatively

significant and representative of completely mixed non-source separated wastewater without flush water inclusion. The impact was not only a restriction in water vapour mass transport but also the induction of wetting, as demonstrated by the permeate quality (Figure 9). The mechanism for wetting is ascribed to surface adsorption, which reduces membrane surface contact angle, subsequently limiting the repulsion of water (30). Goh et al. (12) evidenced the heterogeneity of adsorptive organic surface fouling in MD applied to wastewater. It is asserted that the early breakthrough noted in this study, was induced by discrete areas of the membrane becoming more severely compromised, that could have been exacerbated by the broader more elongated pores within the pore size distribution (Figure 2). The same authors operated MD within a bioreactor for wastewater treatment comprised of biomass and extracellular polymeric substances concentrations of  $6000 \text{ mg l}^{-1}$  and  $150 \text{ mgEPS l}^{-1}$  respectively, and noted negligible breakthrough or flux decline over 25 days of operation, and concluded that it is the chemical nature of the foulant, and not necessarily the concentration, that will determine the rate of wetting (12). This is analogous to the separation of urine in this study in which the concentrative effect of MD did not evidently influence permeate quality (Figure 9). Importantly, whether undertaking water separation from urine or faecally contaminated urine, >95% COD reduction can be achieved with the use of waste heat. However, provided faecal contamination is limited through initial physical separation (8)(14)(24), then permeate quality should exceed the proposed discharge standard for non-sewered sanitation (3) in a single separation step.

#### **4. Conclusions**

The impact of fouling, cleaning and feed water characteristics on the thermally driven membrane separation of water from urine has been investigated to determine the efficacy of membrane distillation as a platform technology for non-sewered sanitation:

- Hydrophobic microporous membranes provide significant single-stage separation that exceeds the proposed non-sewered sanitation discharge standards for ammonia, COD and suspended

solids. It is suggested that operational resilience can be further enhanced through the use of hydrophobic microporous membranes with narrower pore size distribution and more cylindrical pores;

- Whilst surface deposition reduced mass transfer during the treatment of urine, permeate quality was not affected, and the accumulated foulant appeared physically reversible, indicating non-specific binding to the membrane surface. It is proposed that further in-situ optimisation can be achieved through enhanced hydrodynamic control to limit polarisation.
- High organics separation was achieved despite heavy faecal contamination, but this introduced wetting phenomena, which reduced permeate quality and constrained membrane flux. The present study represents the upper limit of faecal contamination. Further investigation into the impact of lesser faecal contamination is warranted to ascertain the extent of upstream separation needed (e.g. source separation, post-flush source separation or pre-filtration) to ensure the discharge standard can be consistently and reliably achieved.
- Consistent permeate quality was produced during the treatment of urine despite concentration exceeding  $C_f$  1.5, which is encouraging. However, concentration management will be required. Synergistic relationships in the literature between bio-treatment and membrane distillation have been demonstrated which warrant evaluation.

### **Acknowledgements**

This publication is based on research funded by the Bill & Melinda Gates Foundation (Grant no. OPP1111272). The findings and conclusions contained within are those of the authors and do not necessarily reflect positions or policies of the funders. Enquiries for access to the data referred to in this article should be directed to: [researchdata@cranfield.ac.uk](mailto:researchdata@cranfield.ac.uk).

### **References**

1. Hutton, G. (2013) Global costs and benefits of drinking-water supply and sanitation

- interventions to reach the MDG target and universal coverage. *J Water Health.*, 11 (1):1–12.
2. Hutton, G.; Haller L. (2004) Evaluation of the Costs and Benefits of Water and Sanitation Improvements at the Global Level. *World Heal Organ.*, 1–87.
  3. American National Standards Institute (ANSI). (2016) Non-Sewered Sanitation Systems: General safety and performance requirements for design and testing. Report No. ISO/PC 305/N008.
  4. Hanak, D.P.; Kolios, A.J.; Onabanjo, T.; Wagland, S.T.; Patchigolla, K.; Fidalgo, B. et al. (2016) Conceptual energy and water recovery system for self-sustained nano membrane toilet. *Energy Convers Manag.*, 126:352–61.
  5. Mercer, E.; Cruddas, P.; Williams, L.; Kolios, A.; Parker, A.; Tyrrel, S. et al. (2016) Selection of screw characteristics and operational boundary conditions to facilitate post-flush urine and faeces separation within single household sanitation systems. *Environ Sci Water Res Technol.*, 2(6):953–64.
  6. Onabanjo, T.; Kolios, A.J.; Patchigolla, K.; Wagland, S.T.; Fidalgo, B.; Jurado, N. et al. (2016) An experimental investigation of the combustion performance of human faeces. *Fuel.*, 184:780–91.
  7. van Voorthuizen, E.; Zwijnenburg, A.; van der Meer, W.; Temmink, H. (2008) Biological black water treatment combined with membrane separation. *Water Res.*, 42(16):4334–40.
  8. Cruddas, P.H.; McAdam, E.J.; Kolios, A.; Parker, A.; Williams, L.; Martin, B. et al. (2015) Biosolids Management Within the Nano Membrane Toilet – Separation, Thickening and Dewatering. In: *WEF/IWA Residuals and Biosolids Conference*. Washington DC, US.

9. Frechen, F.B.; Exler, H.; Romaker, J.; Schier, W. (2011) Long-term behaviour of a gravity-driven dead end membrane filtration unit for potable water supply in cases of disasters. *Water Sci Technol Water Supply.*, 11(1):39–44.
10. Ouma, J.; Septien, S.; Velkushanova, K.; Pocock, J.; Buckley, C. (2016) Characterization of ultrafiltration of undiluted and diluted stored urine. *Water Sci Technol.*, 74(9):2105–14.
11. Edwie, F.; Chung, T.S. (2012) Development of hollow fiber membranes for water and salt recovery from highly concentrated brine via direct contact membrane distillation and crystallization. *J Memb Sci.*, 421–422:111–23.
12. Goh, S.; Zhang, Q.; Zhang, J.; McDougald, D.; Krantz, W.B.; Liu, Y. et al. (2013) Impact of a biofouling layer on the vapor pressure driving force and performance of a membrane distillation process. *J Memb Sci.*, 438:140–52.
13. Zhao, Z.P.; Xu, L.; Shang, X.; Chen, K. (2013) Water regeneration from human urine by vacuum membrane distillation and analysis of membrane fouling characteristics. *Sep Purif Technol.*, 118:369–76.
14. Tun, L.L.; Jeong, D.; Jeong, S.; Cho, K.; Lee, S.; Bae, H. (2016) Dewatering of source-separated human urine for nitrogen recovery by membrane distillation. *J Memb Sci.*, 512:13–20.
15. Grigoriev, A.I.; Sinyak, Y.E.; Samsonov, N.M.; Bobe, L.S.; Protasov, N.N.; Andreychuk, P.O. (2011) Regeneration of water at space stations. *Acta Astronaut.*, 68(9–10):1567–73.
16. Franken, A.C.M.; Nolten, J.A.M.; Mulder, M.H. V.; Bargeman, D.; Smolders, C.A. (1987) Wetting criteria for the applicability of membrane distillation. *J Memb Sci.*, 33(3):315–28.

17. Autin, O.; Hai, F.; Judd, S.; McAdam, E.J. (2016) Investigating the significance of coagulation kinetics on maintaining membrane permeability in an MBR following reactive coagulant dosing. *J Memb Sci.*, 516:64–73.
18. Meng, S.; Ye, Y.; Mansouri, J.; Chen, V. (2014) Fouling and crystallisation behaviour of superhydrophobic nano-composite PVDF membranes in direct contact membrane distillation. *J Memb Sci.* 463:102–12.
19. Chiam, C.K.; Sarbatly, R. (2014) Vacuum membrane distillation processes for aqueous solution treatment-A review. *Chem Eng Process Process Intensif.*, 74:27–54.
20. Putman, D.F. (1971) Composition and Concentrative Properties of Human Urine. *NASA Contract Rep.*, (July):109.
21. Mills, C.O.; Ellas, E.; Martin, G.H.B.; Woo, M.T.C.; Winder, A.F. (1988) Surface Tension Properties of Human Urine: Relationship with Bile Salt Concentration. *J Clin Chem Clin Biochem.*, 26(4):187–94.
22. Julian, H.; Meng, S.; Li, H.; Ye, Y.; Chen, V. (2016) Effect of operation parameters on the mass transfer and fouling in submerged vacuum membrane distillation crystallization (VMDC) for inland brine water treatment. *J Memb Sci.*, 520:679–92.
23. Cath, T.Y.; Adams, D.; Childress, A.E. (2005) Membrane contactor processes for wastewater reclamation in space: II. Combined direct osmosis, osmotic distillation, and membrane distillation for treatment of metabolic wastewater. *J Memb Sci.*, 257(1–2):111–9.
24. Gryta, M. (2008) Fouling in direct contact membrane distillation process. *J Memb Sci.*, 325(1):383–94.
25. Lim, S.K.; Goh, K.; Bae, T-H.; Wang, R. (2017) Polymer-Based Membranes for Solvent-Resistant Nanofiltration: A Review. *Chinese J Chem Eng.*

26. Giri, D. (2015) Calcium phosphate crystals in urine. *Medical labs.*, [cited 2017 Aug 1]. Available from: <http://www.medical-labs.net/calcium-phosphate-crystals-in-urine-3109/>
27. Metzger, U.; Le-Clech, P.; Stuetz, R.M.; Frimmel, F.H.; Chen, V. (2007) Characterisation of polymeric fouling in membrane bioreactors and the effect of different filtration modes. *J Memb Sci.*, 301(1–2):180–9.
28. Achilli, A.; Cath, T.Y.; Marchand, E.A.; Childress, A.E. (2009) The forward osmosis membrane bioreactor: A low fouling alternative to MBR processes. *Desalination.*, 238(1–3):10–21.
29. Qin, J.J.; Kekre, K.A.; Oo, M.H.; Tao, G.; Lay, C.L.; Lew, C.H. et al. (2010) Preliminary study of osmotic membrane bioreactor: Effects of draw solution on water flux and air scouring on fouling. *Water Sci Technol.*, 62(6):1353–60.
30. McLeod, A.; Jefferson, B.; McAdam, E.J. (2014) Biogas upgrading by chemical absorption using ammonia rich absorbents derived from wastewater. *Water Res.*, 67:175–86.

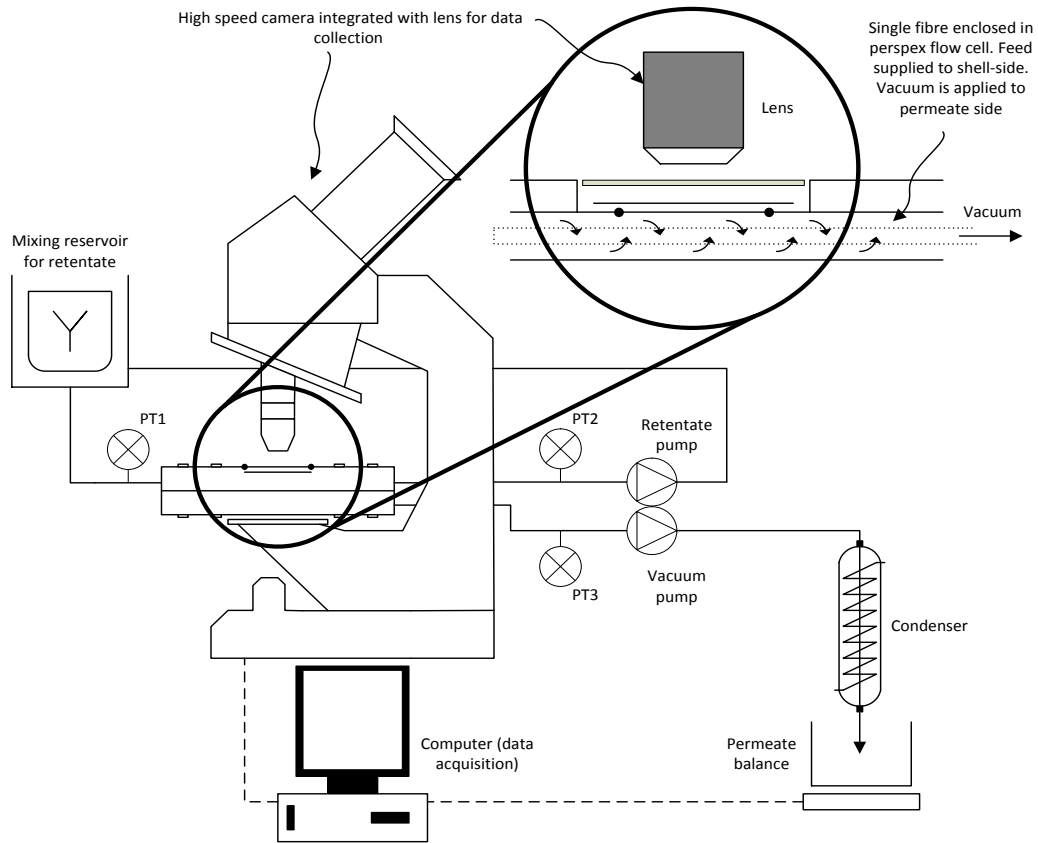


Figure 1. Experimental set-up.

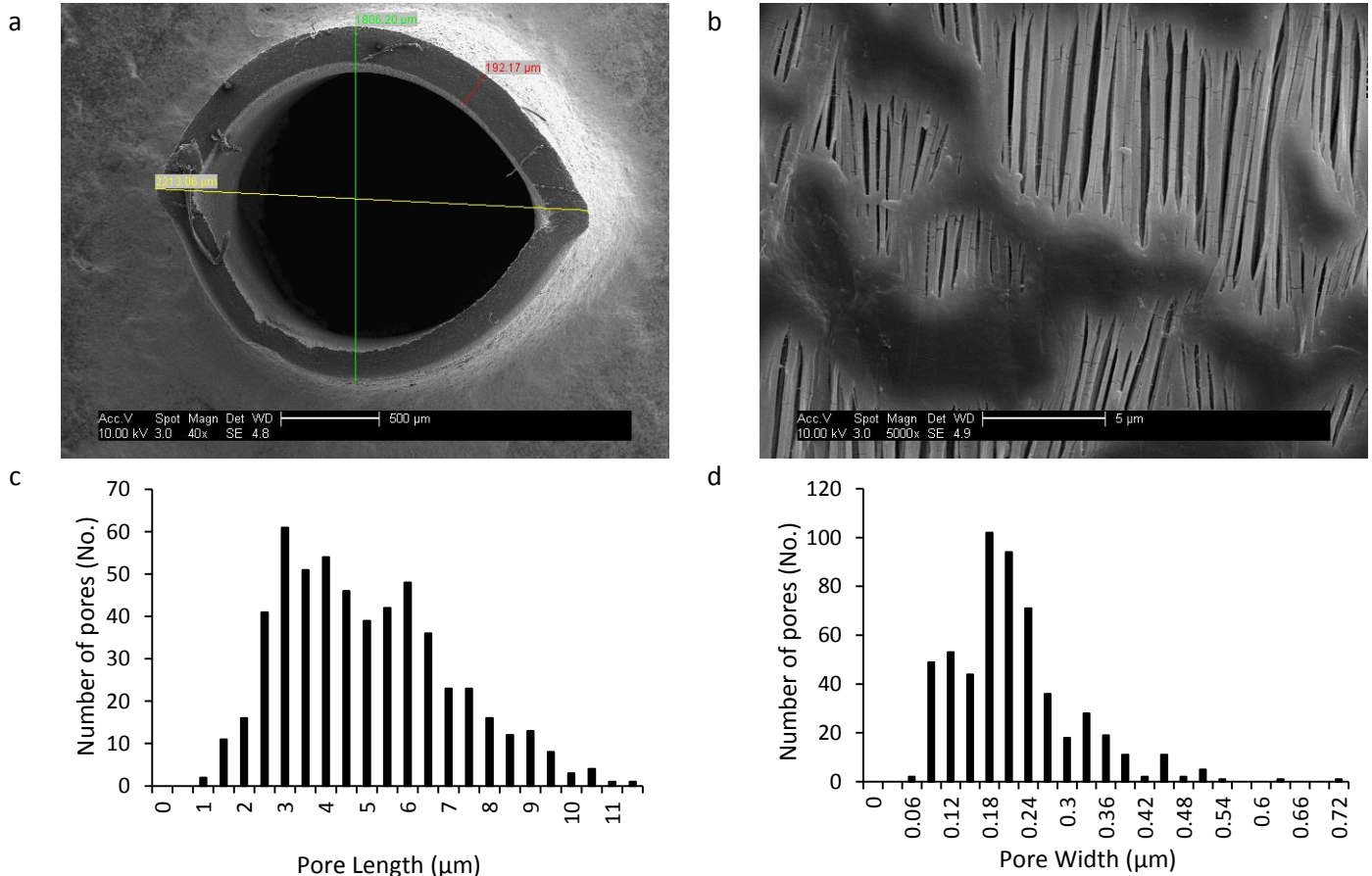


Figure 2. PTFE Hollow fibre characterisation: (a) Lumen diameter/wall thickness; (b) Pore structure; (c) Pore length characterisation ( $n = 550$ ); (d) Pore width characterisation ( $n = 550$ ). Images (a) and (b) taken using scanning electron microscopy (Acceleration Voltage, 10 kV).



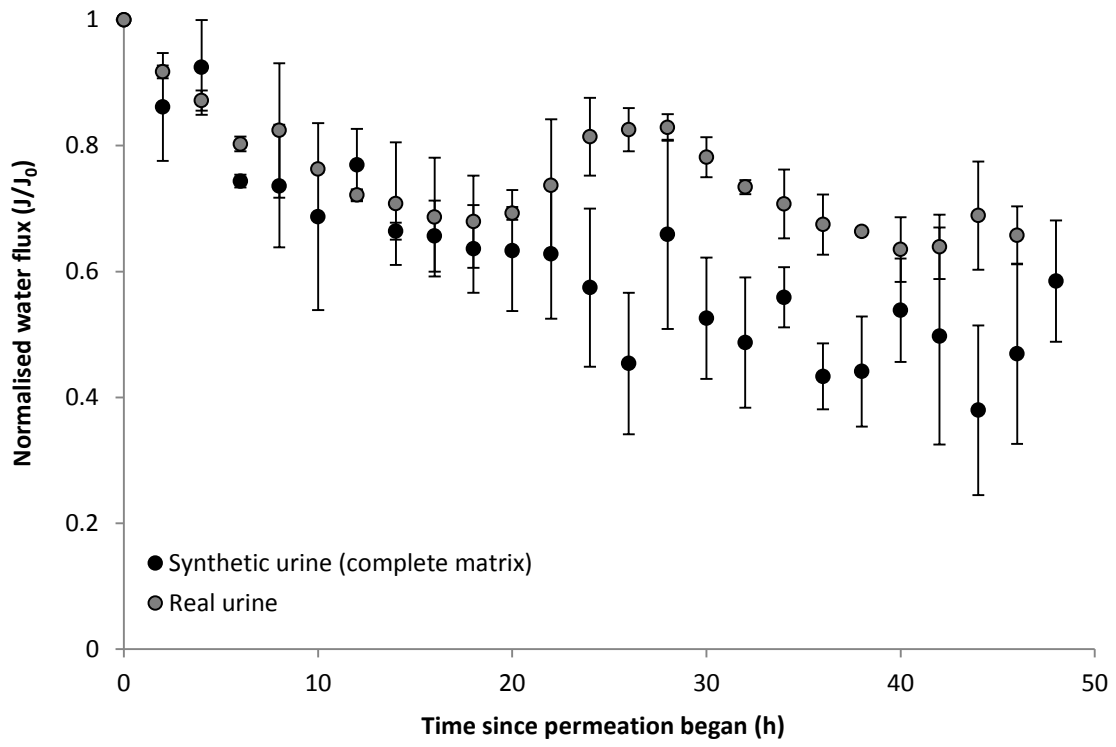


Figure 3. Flux variation during the vacuum membrane distillation of real urine. Feed temperature= 60 °C, Cross flow velocity = 0.11 m s<sup>-1</sup>, Initial flux  $J_0$ = 3.05 L m<sup>-2</sup> h<sup>-1</sup>, vacuum degree= 40 mBarA.

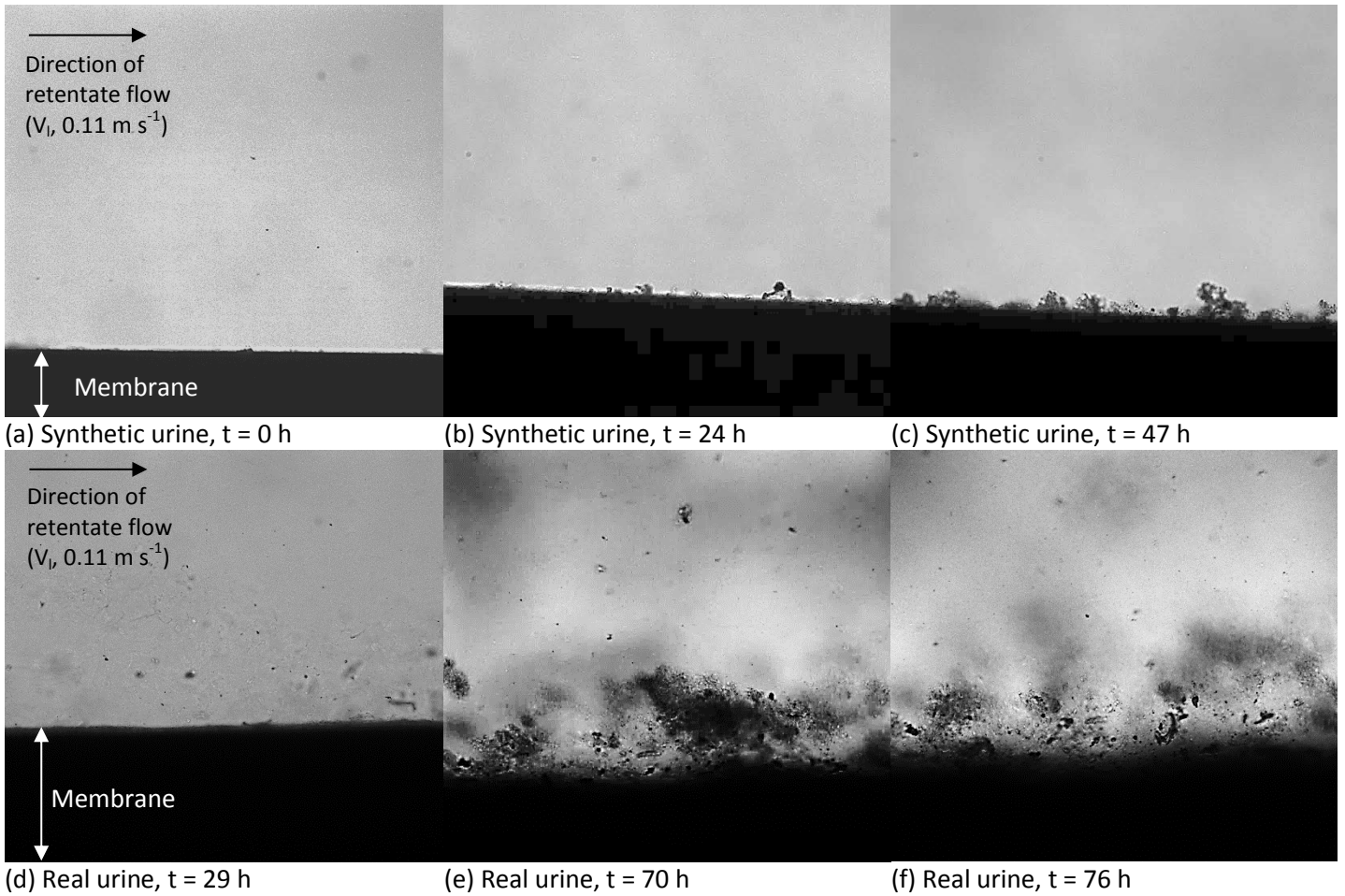


Figure 4. Direct observation images collected in real-time, provide illustrative evidence of the difference in fouling behaviour that the two solutions introduce to the membrane surface during membrane distillation: (a-c) Synthetic urine; (d-f) Real urine.

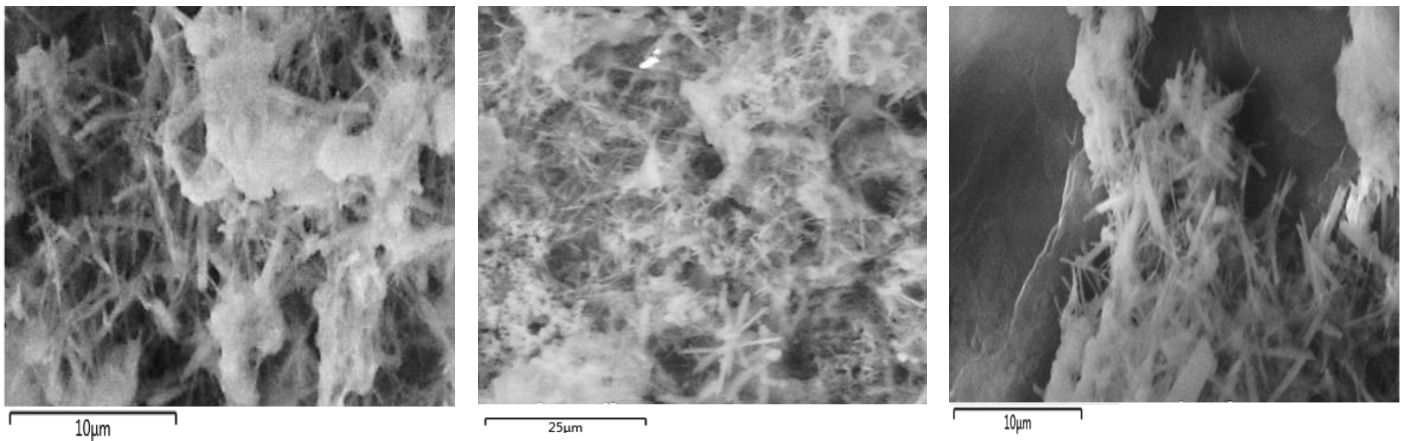


Figure 5. SEM observations of the membrane surface after 96h of operation. Feed temperature=  $60^\circ\text{C}$ , cross flow velocity =  $0.11 \text{ m.s}^{-1}$ , vacuum degree= 40 mBar:

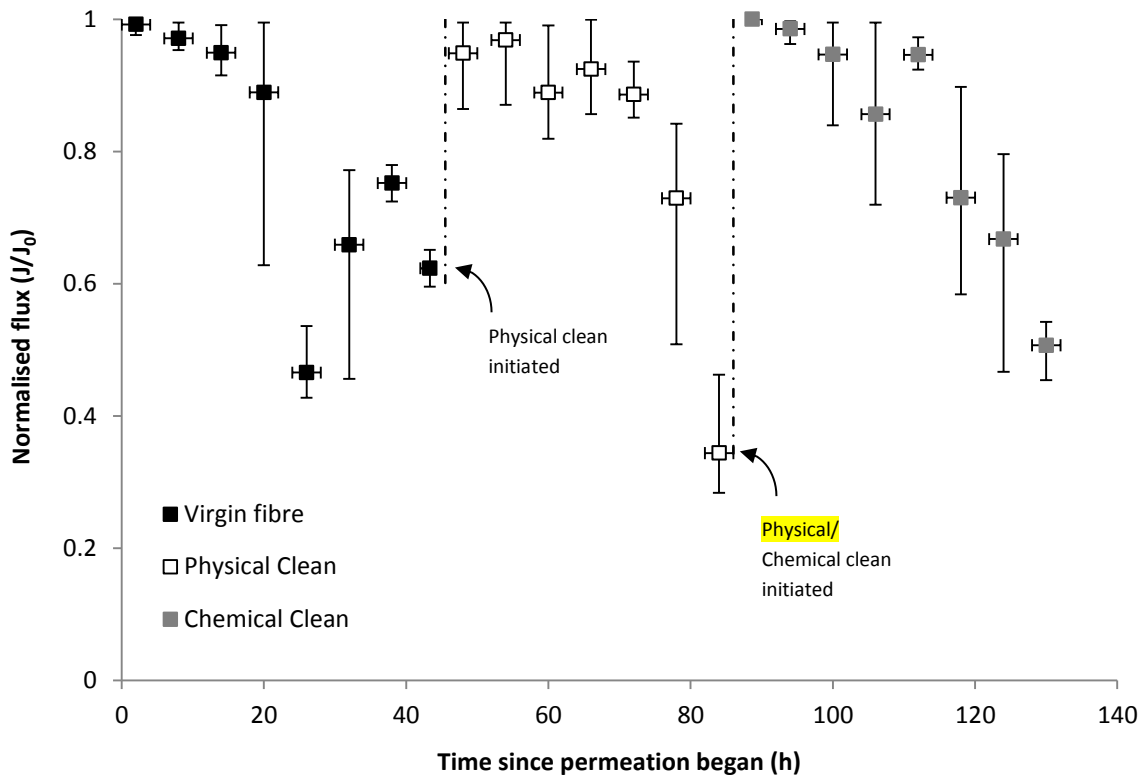


Figure 6. Flux variation during the VMD of real urine using a virgin membrane, physically cleaned with deionised water and chemically cleaned.

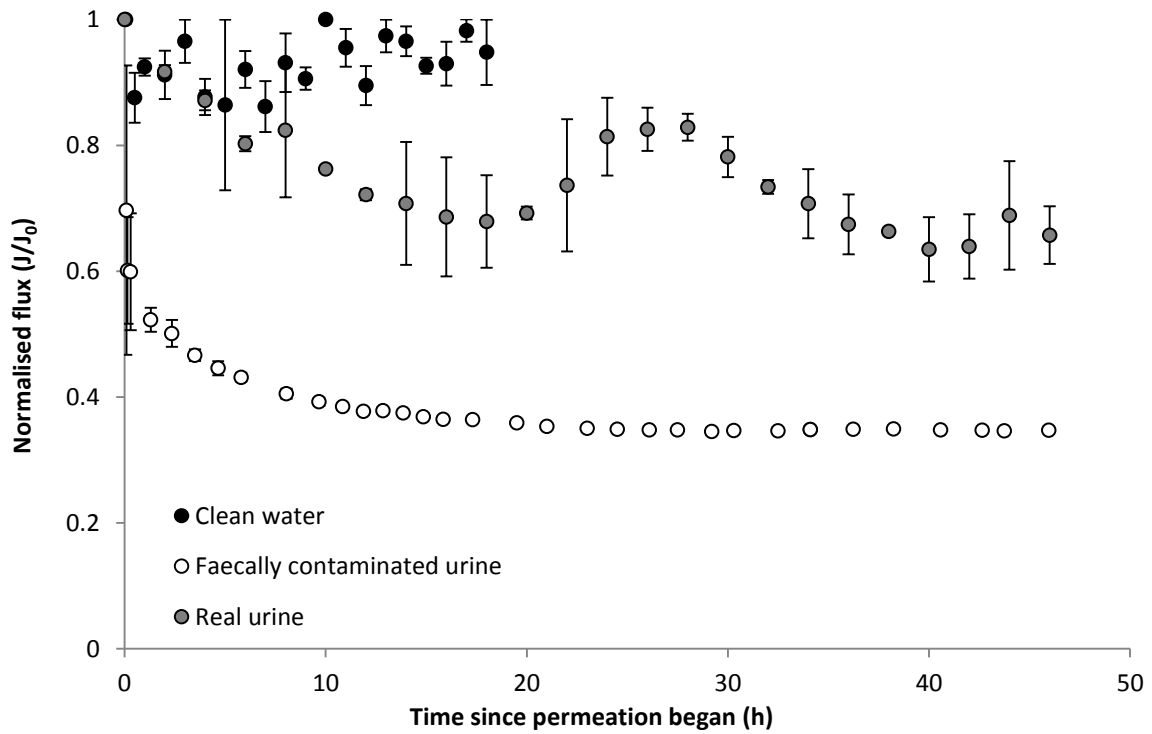


Figure 7. Comparison of flux data for urine, faecally contaminated urine and microfiltration (MF) pre-treated faecally contaminated urine. Feed temperature 60°C, vacuum pressure 45 mbar.

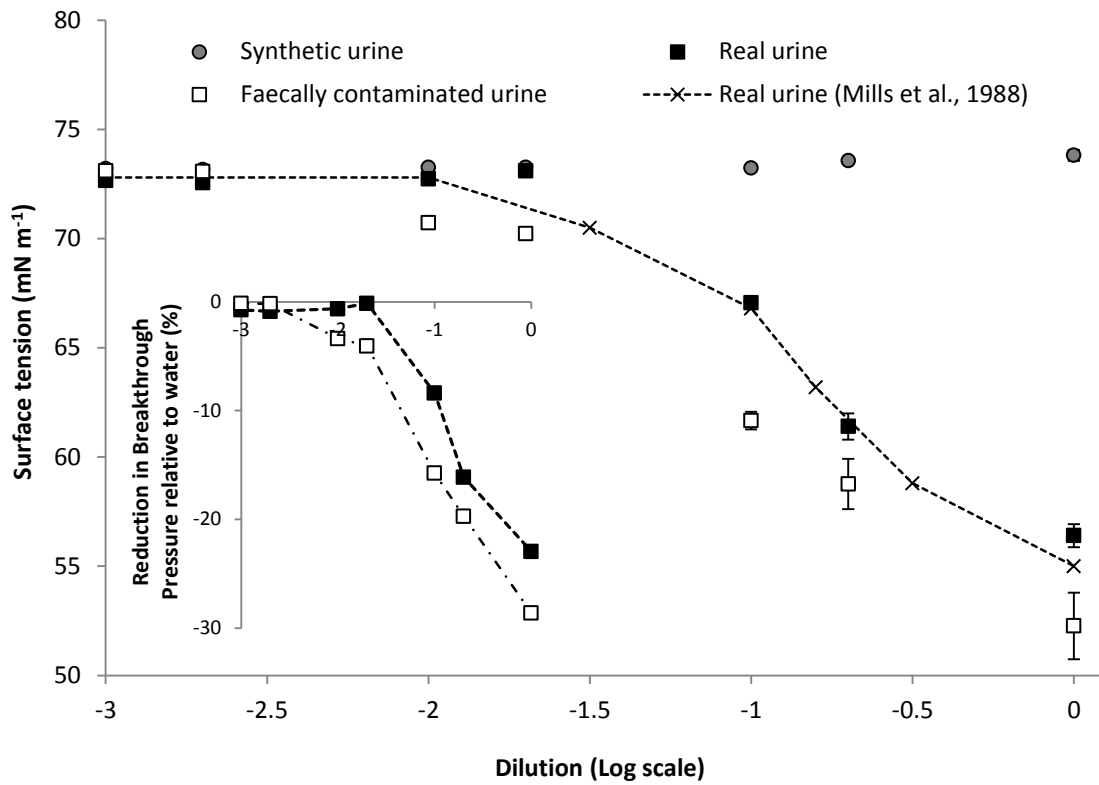


Figure 8. Surface tension data for urine, faecally contaminated urine and microfiltration (MF) pre-treated faecally contaminated urine. Inset: zoom into transitional region.

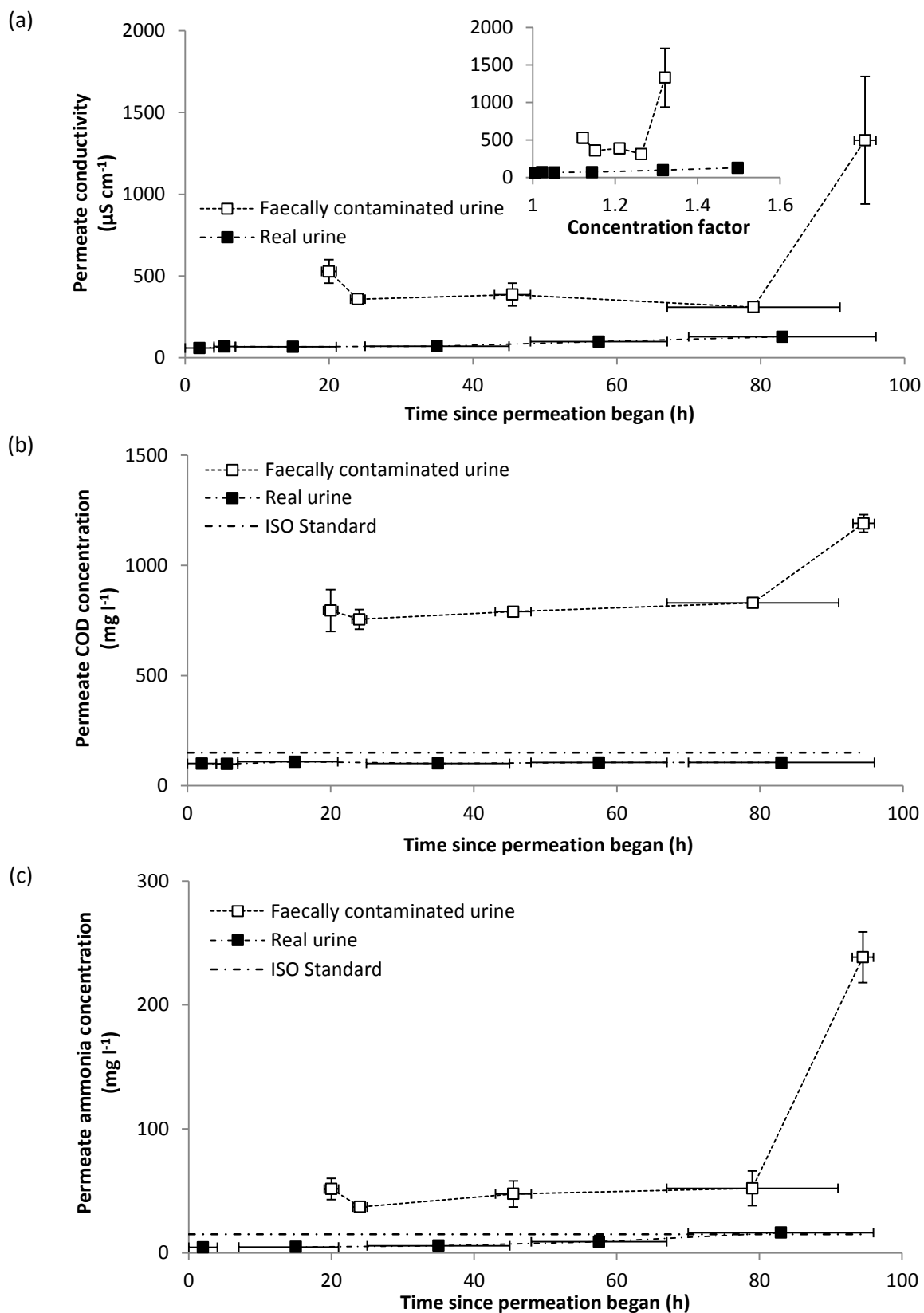


Figure 9. Produced permeate quality: (a) Conductivity, inset with concentration factor; (b) COD, compared to ISO discharge standard ( $150 \text{ mg l}^{-1}$ ); (c) Ammonia, compared to proposed ISO discharge standard ( $\text{TN } 15 \text{ mg l}^{-1}$ ). Initial urine concentration:  $9.4 \text{ mS cm}^{-1}$ ,  $6470 \text{ mgCOD l}^{-1}$ ,  $244 \text{ mgNH}_4 \text{ l}^{-1}$ . Initial faecally contaminated urine concentration:  $17.5 \text{ mS cm}^{-1}$ ,  $20400 \text{ mgCOD l}^{-1}$ ,  $900 \text{ mgNH}_4 \text{ l}^{-1}$

Table 1. Membrane rejection following 96 h filtration of synthetic and real urine: Feed temperature, 60 °C;  $V_L$ , 0.11 m s<sup>-1</sup>; Vacuum, 40mBarA,  $C_f$  = feed concentration,  $C_p$  = permeate concentration.

Feedwater	Conductivity (mS cm <sup>-1</sup> )			COD (mg L <sup>-1</sup> )			Ammonium (mg L <sup>-1</sup> )			Urea (mg L <sup>-1</sup> )			Creatine (mg L <sup>-1</sup> )			Creatinine (mg L <sup>-1</sup> )		
	$C_f$	$C_p$	%	$C_f$	$C_p$	%	$C_f$	$C_p$	%	$C_f$	$C_p$	%	$C_f$	$C_p$	%	$C_f$	$C_p$	%
Synthetic Urine																		
<i>Inorganic salts</i>	20.0	0.02	99.9	-	-	-	-	-	-	-	-	-	-	-	-	-	-	-
<i>Inorganic salts + Organic Salts</i>	20.4	0.02	99.9	1970	55	97.2	-	-	-	-	-	-	-	-	-	-	-	-
<i>Inorganic salts + Organic Salts + NH<sub>4</sub> salts</i>	19.0	0.08	99.6	1860	43	97.7	106	8	92.4	-	-	-	-	-	-	-	-	-
<i>Inorganic salts + Organic Salts + NH<sub>4</sub> salts + Urea</i>	20.6	0.16	99.2	5060	66	98.7	216	14	93.5	-	-	-	-	-	-	-	-	-
Real Urine	18.4	0.26	98.6	6470	104	98.4	244	18	92.5	12437	12	99.9	5	0.1	97.8	100	0.1	99.9

Table 2. Composition of the cleaning fractions following filtration of real urine (50 mL rinse solution)

		Conductivity (μS cm <sup>-1</sup> )	COD (mg l <sup>-1</sup> )	COD (g m <sup>-2</sup> )
<i>Physical cleaning</i>	DI water	2190	772	6.8
<i>Chemical cleaning</i>	DI water	2530	527	4.6
	Citric acid	308	187	1.6
	NaOH	22	143	1.3
	DI water	16	149	1.3

Table 3. Membrane rejection at 48h filtration following various cleaning protocols

	Conductivity (μS cm <sup>-1</sup> )	NH <sub>4</sub> <sup>+</sup> -N (mg l <sup>-1</sup> )	COD (mg l <sup>-1</sup> )
<i>Initial</i>	99.1	98.2	99
<i>Physical cleaning</i>	98.4	97	98.6
<i>Chemical cleaning</i>	97.6	95.3	98.4